GEOCHEMICAL SIGNATURES OF GNEISS SAMPLES FROM ONZON, THABEIKKYIN AND SAGAING AREAS: IMPLICATIONS FOR PROTOLITH COMPOSITION, SOURCE–AREA WEATHERING AND DEPOSITIONAL TECTONIC SETTING

Ye Kyaw Thu[1] and Maw Maw Win[2]

Abstract

The Cenozoic Mogok metamorphic belt exposed at the western margin of the Shan-Thai Block consists of metaigneous and metasedimentary rocks with various granitoid intrusions. The common mineral assemblages of gneiss samples are characterized by garnet + biotite + plagioclase + K-feldspar + quartz with cordierite and sillimanite in some samples forming under upper amphibolite to granulite facies conditions. Geochemical data were used to evaluate the possible protolith composition, sourece–area weathering, provenance and tectonic setting of the gneiss samples. Sagaing samples are more enriched in Fe relative to Onzon and Thabeikkyin samples. Compared with average crustal content the samples show similar composition with depletion of CaO, Na_2O, P_2O_5, Sr and Nb and enrichment of Rb, Y and Th. Evidences form major and trace element concentrations, ratios and use of various diagrams point to the derivation of Onzon and SM2 unit samples from psammitic composition mainly greywacke and SM1 unit sample from pelitic compositions except for Thabeikkyin sample, which has felsic igneous protolith. In addition, Chemical Index of Alteration (CIA), Chemical Index of Weathering (CIW), Index of compositional Variability (ICV) values and major element diagrams indicate that the source areas had undergone moderate to high degree of weathering. Based on the major and trace variation sediment deposition might have occurred at passive margin and active continental margin.

Keywords: geochemistry, protolith, source–area weathering, tectonic setting

Introduction

The compositions of the deep crustal metamorphic rocks are vital to decipher the lower crust and its protolith composition (Rudnick, 1992; Rollinson, 2012). Analyses of major, trace and rare earth elements concentration from metamorphosed rocks can reveal the details of protolith compositions, which cannot be determined in thin sections. The behavior of certain trace elements and products of their metamorphism can be considered as indicators of the continental crust composition, and the geochemical record of these rocks provides a key for understanding their evolution.

The Cenozoic Mogok metamorphic belt is sited at the western margin of the Shan-Thai Block and consists of metaigneous and metasedimentary rocks with various granitoid intrusions. These metamorphic rocks were regionally metamorphosed under medium- to high-grade amphibolite facies and localized granulite facies conditions, and has been estimated as Paleogene and younger in age (Bertrand et al., 1999, 2001; Barley et al., 2003; Mitchell et al., 2007; Searle et al., 2007; Yonemura et al., 2013; Maw Maw Win et al., 2016; Ye Kyaw Thu et al., 2016, 2017). Although, the Mogok metamorphic belt has been investigated by many previous studies, the geochemical signatures of the metasediments from the belt are very poorly constrained. The present study attempts to decipher the geochemical characteristics of gneiss samples from Onzon, Thabeikkyin and Sagaing areas in the middle segment of the Mogok metamorphic belt, and to place constraints on the composition and nature of the source rocks (provenance) and the tectonic setting for their deposition.

[1] Dr, Lecturer, Department of Geology, University of Magway
[2] Dr, Associate Professor, Department of Geology, Lashio University

Geology of the Onzon, Thabeikkyin and Sagaing Areas

Onzon and Thabeikkyin areas located 100 km north of the Mandalay region are dominated by high-grade paragneisses with various types of marbles and calc-silicate rocks (Fig. 1a). In the sampling area the marbles and calc-silicate rocks are well exposed and locally intruded by granitoid rocks. Major lithologies of the Onzon area include garnet–cordierite gneiss, garnet–biotite gneiss, and biotite gneiss. The gneiss samples contain the common mineral assemblage of garnet–biotite–plagioclase–K-feldspar–quartz with cordierite and sillimanite in some samples. In the Thabeikkyin area, the main rock type is highly weathered garnet–biotite gneiss, and show similar mineral assemblages as Onzon area. Ye Kyaw Thu et al. (2016, 2017) reported the pressure and temperature (*P*–*T*) conditions of 0.60–0.78 GPa/800–860 °C using a conventional geothermobarometers for the peak metamorphic stage from these areas.

In Sagaing area, the Mogok metamorphic rocks, which are locally named the Sagaing metamorphic rocks, are mainly composed of gneiss, marble, calc-silicate rock, schist, and amphibolite. The Mogok metamorphic rocks from the area are divided into Sagaing Metamorphic Unit 1 (SM1) and Sagaing Metamorphic Unit 2 (SM2), which are gneiss-dominant units that interleave layers of amphibolite and calc-silicate rock/marble, respectively (Fig. 1b). The SM samples are characterized by common mineral assemblages of garnet, biotite, plagioclase, K-feldspar, quartz, and graphite with sillimanite in some samples. The pressure and temperature (*P*–*T*) conditions were suggested 0.58–1.0 GPa/780–850 °C using a conventional geothermobarometers (Maw Maw Win et al., 2016).

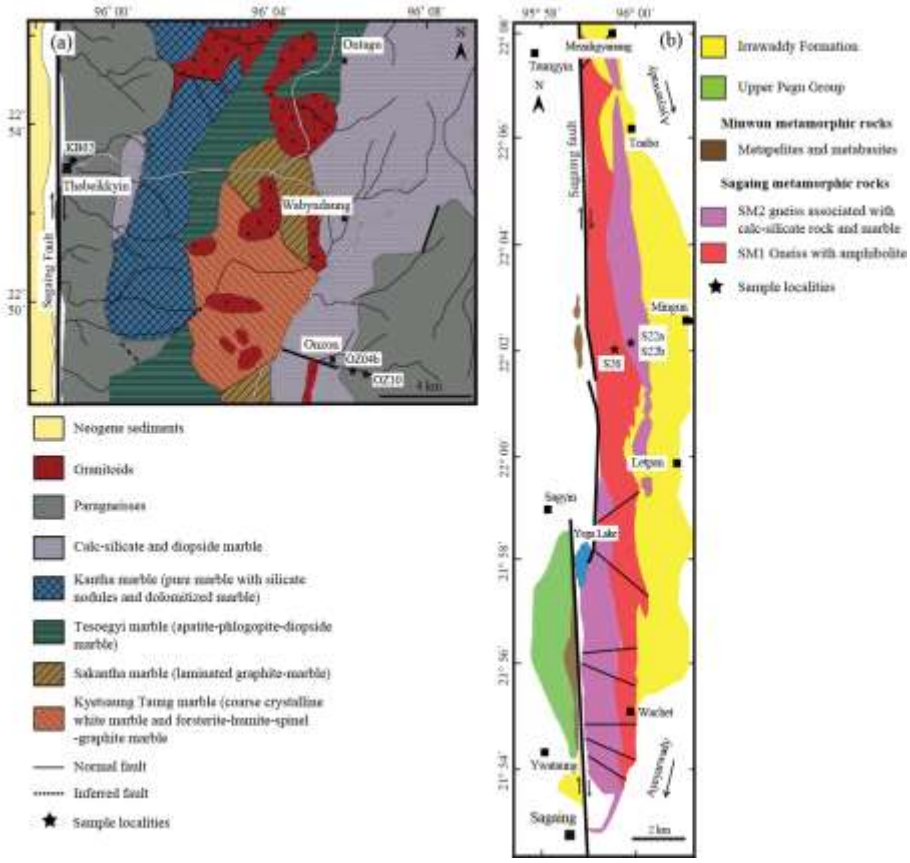

Figure 1 Geological map showing the major rock units of (a) Onzon and Thabeikkyin areas (after Myint Liwin Thein et al., 1990) and (b) Sagaing area (Maw Maw Win et al., 2016).

Petrography

The garnet–cordierite gneiss (OZ04b sample) and garnet–biotite gneisses (OZ10 sample) were collected from Onzon area (longitude 96° 06' 05″E, latitude 22° 48' 42″N; Fig. 1a), and the garnet-biotite gneiss (KB02 sample) were from Thabeikkyin area (longitude 95° 58' 59" E, latitude 22° 53' 18" N; Fig. 1a). S26 sample was collected form SM1 (95° 59' 18″ E, 22° 02' 01″ N; Fig. 1b), and S22a and S22b samples were from SM2 (95° 59' 57″ E, 22° 02' 12″ N; Fig. 1b). These samples were selected for detailed geochemical analysis, and OZ for OZ04b and OZ10 samples, KB for KB02 sample, SM1 for S26 sample and SM2 for S22a and b samples are here used for abbreviation. Abbreviations for minerals and end-members are after Whitney and Evans (2010).

All samples are characterized by garnet, biotite, plagioclase, K-feldspar, sillimanite and quartz with minor rutile, ilmenite, graphite and zircon with cordierite in OZ04b sample. Garnet grains occur as subhedral to anhedral porphyroblasts ranging in size from 2–5 mm in diameter (Fig. 2). Some garnets contain fine grains of sillimanite, cordierite, and quartz inclusions in OZ04b sample (Fig. 2a) and acicular sillimanite, biotite and quartz grains in OZ10, S26, S22a and b sample (Figs. 2c and d). Some garnet grains are partially replaced by secondary biotite and muscovite-rich aggregates along cracks. The cordierite in Sample OZ04b commonly contains symplectitic grains of quartz, rare spinel and biotite (Figs. 2a and b). Biotite grains occur as an inclusion phase in garnet and cordierite, as isolated phase in matrix and as intergrown phase with cordierite and quartz. Plagioclase and K-feldspar occur as primary phase in all samples (Fig. 2). In OZ04b and S26 samples, rutile occurs as isolated grain and intergrowth grains with ilmenite in the matrix (Fig. 2b). Spinel grains occur as symplectitic phase with cordierite in OZ04b sample (Fig. 2a). Prismatic sillimanite grains occur as matrix phase and inclusion in garnet (Fig. 2). Graphite, ilmenite, zircon, monazite and apatite occur as accessory phases in all samples.

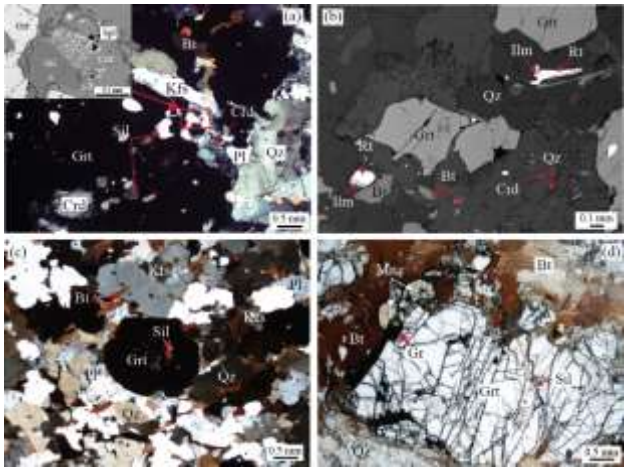

Figure 2 photomicrographs showing (a) garnet porphyroblast with inclusions of cordierite and sillimanite and symplectitic cordierite grian with spinel (OZ04b sample), (b) Back Scattered Electron (BSE) image of the symplectitic cordierite grain with quartz and biotite and intergrown rutile grain with ilmenite (OZ04b sample), (c) garnet grains with sillimanite inclusion (OZ10 sample) and (d) garnet grain and primary monazite (S26 sample).

Geochemistry

Analytical Procedures

Sample were made for the detailed study of the constituent mineral assemblages under polarizing microscope and were made powder and dried in the oven to dry out the water in the sample. Dried samples were weighed and placed in the microfurnace setting 950 °C for 5 hours. The glass beads were then prepared by fusing mixtures of powder samples and $Li_2B_4O_7$ in a weight ratio of 0.7:6.0. Whole-rock compositions used for the geochemical analysis were determined by an X-ray fluorescence spectrometer (XRF; Rigaku ZSX Primus II equipped with a Rh X-ray tube operated at 60 kV and 50 mA) at Nagoya University. Sedimentary and igneous rock reference samples issued by the Geological Survey of Japan (GSJ) were used for the calibration. Whole rock chemical analyses of studied samples are listed in table 1.

Table 1 Analysis of the major and trace elements of the analyzed samples

Sample	OZ04b	OZ10	KB01	S26	S22a	S22b
SiO_2	69.99	73.91	64.51	51.73	67.45	62.58
TiO_2	0.84	0.67	0.64	1.32	0.67	0.80
Al_2O_3	12.38	11.06	16.35	18.61	12.58	14.90
Fe_2O_3*	6.33	5.38	5.78	13.19	7.91	7.93
MnO	0.09	0.09	0.14	0.19	0.14	0.11
MgO	3.48	2.62	2.05	5.51	3.17	3.28
CaO	1.34	1.03	2.46	2.33	1.46	1.45
Na_2O	1.76	1.99	2.64	1.42	1.46	1.15
K_2O	2.35	2.49	4.80	3.42	3.52	5.86
P_2O_5	0.07	0.06	0.06	0.10	0.05	0.10
LOI	1.08	1.32	1.04	1.44	2.39	1.07
Total	99.71	100.62	100.47	99.26	100.80	99.23
Nb	13.1	1.08	4.30	57	31	33
Zr	279	191	178	272	279	232
Th	21	15.2	22.0	64.8	35.2	31.9
Y	38.2	23.9	29.0	77	58	48
Sr	88.6	52.6	251	181	305	158
Pb	13.7	10.0	27.1	33	22	40
Ba	358	621	1020	635	900	883
Rb	108	93.6	134	149	120	249
Cr	123	81.7	69.1	195	97	96
Ni	53.8	37.0	19.8	57	31	33
Zn	70.5	51.3	46.4	163	67	92
Co	19.8	29.5	28.4	30	17	19

* Fe_2O_3 as total Fe

Major, Transition and Trace Elements

The analyzed sample shows a range of SiO_2 (51.7 – 73.9 wt%), Al_2O_3 (11.1–18.6 wt%), MgO (2.1–5.5 wt%), Fe_2O_3 (5.4–13.2 wt%), CaO (1.0–2.5 wt%), Na_2O (1.2–2.6 wt%) and K_2O (2.3–5.9 wt%) (Table 1). X_{Fe} [= FeO/(FeO + MgO + MnO)] ranges from 0.64–0.66 for OZ samples, 0.73 for KB02 sample, 0.70 for S26 sample and 0.70–0.71 for SM2 samples and X_{Al} [= (Al_2O_3 – $3K_2O$)/(Al_2O_3 – $3K_2O$ + FeO + MgO + MnO)] ranges from 0.31–1.25 for OZ sample, 0.20 for KB02 sample, 0.31 for S26 sample and 0.15 – 0.31 for SM2 samples. OZ samples are more enriched in SiO_2 (69.99 – 73.91 wt%). KB and SM samples are more enriched in Al_2O_3 and K_2O compared with OZ samples, and S26 sample shows high TiO_2 value (1.32 wt%). Figure 3 shows depletion in Al_2O_3 for OZ and SM2 samples but similar variation for KB and SM1 sample (Fig. 3a) compared with average shale and arenite composition. MgO are enriched in OZ and SM samples (Fig. 3b). Fe_2O_3 is enriched in SM samples, and OZ, and KB samples have similar variation (Fig. 3c). For Na and K, OZ and most SM samples show slight variation, and KB and S22b sample show enrichment (Fig. 3d).

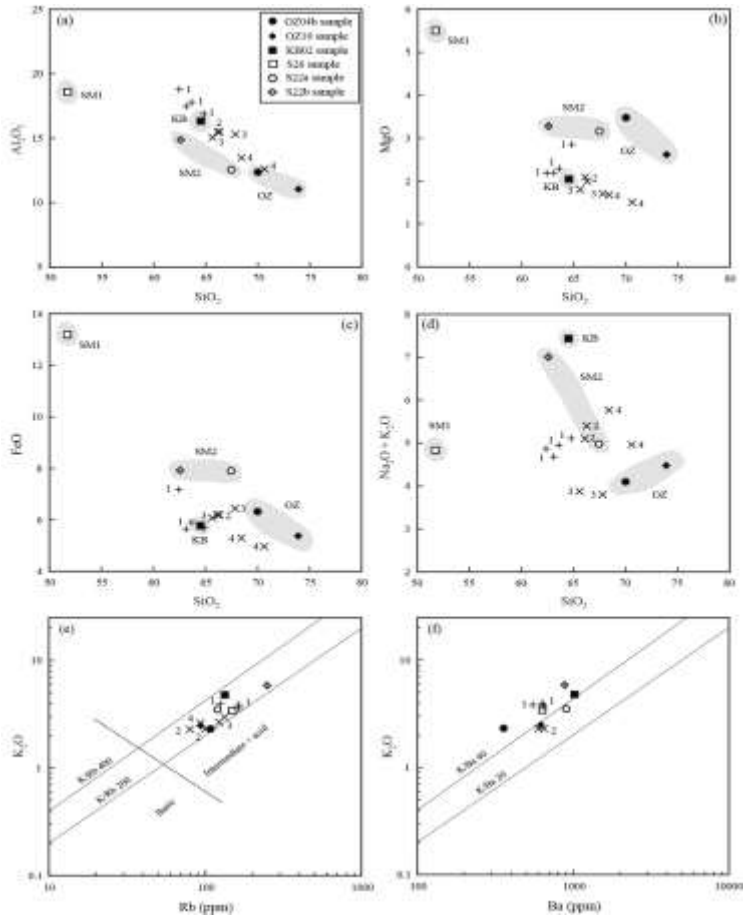

Figure 3 Geochemical variation diagrams for major and trace elements of the studied samples compared with average arenite and shale composition. 1 is average Proterozoic and Phanerozoic cratonic shale composition (Codie, 1993), Post–Archean Australian Shale (PAAS) (Taylor and McLennan, 1985 and McLennan 2001), and North American Shale Composition (NASC) (Gromet et al. 1984); 2 is average Paleozoic and Meso-Cenozoic greywacke composition (Codie, 1993); 3 is average lithic arenite (Argast and Donnelly, 1987) and 4 is feldspathic arenite (Argast and Donnelly, 1987). Boundary line between acid/intermediate and basic compositions in figure (e) is after Floyd and Leveridge (1987).

In figure 3e, the ranges in Rb concentration of S26 and S22a samples are nearly similar in composition with average shale and those of OZ samples are consistent with the greywacke composition. In KB sample the Rb range is near to that of the shale but deviate from it in Ba content (Fig. 3f). The K/Rb ratio for studied samples ranges from 217 to 294 ppm falling within normal field (K/Rb <300 ppm) except KB02 sample (360 ppm).

Spider diagram was made to identify the nature of protolith by normalizing all the analyzed elements to the upper continental crust (UCC) values of Rudnick and Gao (2003) (Fig. 4). The major and minor oxides have a similar composition relative to the UCC, but CaO, Na_2O and P_2O_5 show a slight depletion. Cr, Zn and Co contents show similar concentration to the UCC, and Ni show slight enrichment in OZ04b and S26 sample. For the large ion lithophile elements (LILE) Rb show enrichment for all samples but Sr is significantly depleted in OZ samples and Ba and Pb scatter around the UCC (Fig. 4). The concentration of the high field strength elements (HFSE) shows similar Zr contents, slight enrichment in Y and Th, and significant depletion in Nb, for OZ10 and KB02 samples. These concentrations are most likely to be controlled by the contents of the clay minerals and detrital accessories in the sedimentary protolith (Varga and Szakmány, 2004).

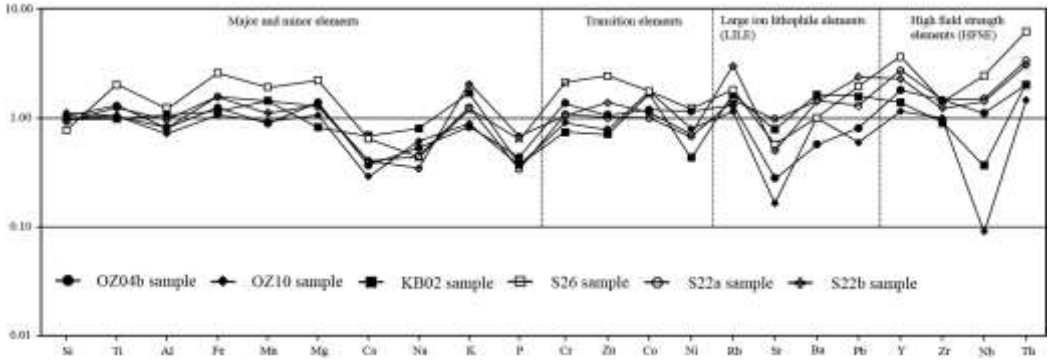

Figure 4 Bulk-rock composition of the analyzed samples plotted in an upper continental crust (UCC) normalized multi-element diagram. UCC data are from Rudnick and Gao (2003).

Discussion

Protolith Composition

The protolith of the studied samples was deduced based on geochemistry. Discriminant function, DF = 10.44 – 0.21SiO_2 – 0.32Fe_2O_3 (total Fe) – 0.98 MgO + 0.55 CaO + 1.46 Na_2O + 0.54K_2O (Shaw 1972) can be deduced to determine whether the protolith is igneous or sedimentary in origin. Positive DF values are regarded as igneous parentage while negative values are of sedimentary origin. OZ and SM samples show negative DF values ranging from −4.55 to −5.14 suggesting a sedimentary origin. However, KB sample show positive DF value of 0.83 suggesting an igneous origin. In log (SiO_2/Al_2O_3) versus log (Fe_2O_3/K_2O) diagram of Herron, 1988 all sample fall within wacke field except S26 sample which fall in slightly Fe-rich shale (Fig. 5a). This is supported by the classification diagram of Wimmenauer (1984) and all samples fall within greywacke and arkose field except for SM1 sample which drop in shale field (Fig. 5b). In addition, the discrimination ratio of 100 x TiO_2/Zr (wt.%/ppm), which are assumed to have a steady behaviour during metamorphism, is lower than 0.4 except S26 sample (0.48), which has shale protolith composition, and suggest to an input of psammitic material to the precursor sediment (Garcia et al., 1991). The Sr value of 53–89 ppm (OZ samples), 251 ppm (KB sample) and 158–305 ppm (SM samples) is consistent with the range of 20–360 ppm (shale) and 100–400 ppm (greywacke). K_2O and Ba are positively correlated (Fig. 3f) and K/Ba ratio of the samples ranges from 39–66 ppm consistent with the range of average shale and greywacke.

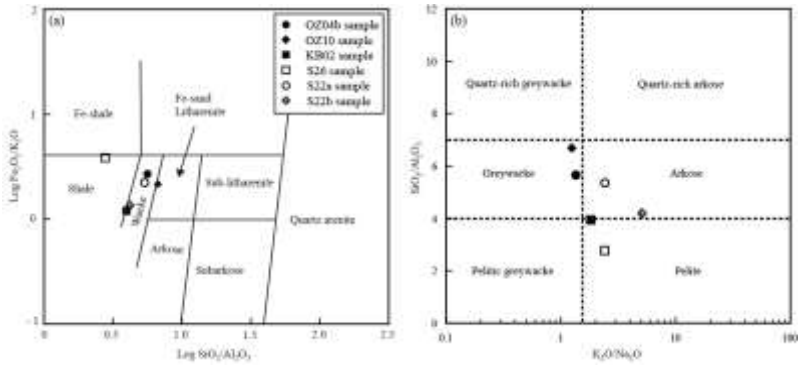

Figure 5 (a) log (SiO_2/Al_2O_3) – log (Fe_2O_3/K_2O) diagram (after Herron, 1988) and (b) K_2O/Na_2O ration and SiO_2/Al_2O_3 ratio diagram (after Wimmenauer, 1984).

The Al_2O_3/TiO_2 ratio of Girty et al. (1996) shows 26 for KB02 sample indicating a source with average andesitic to rhyodacitic composition. KB sample is rich in Al_2O_3 (16.35%), CaO (2.46%), Na_2O (2.64%) and K_2O (4.80%) and low SiO_2 (64.51%) and MgO (2.05%) (Table 1). In these respects, they are similar in composition to tonalite or granodiorite in major element composition. These features suggest that if the KB02 sample has igneous rather than sedimentary protolith, it is consistent with felsic igneous source rocks. In addition, Th/Co ratio (0.78 ppm) and Th/Cr ratio (0.32 ppm) of KB02 sample are consistent with the range of felsic source 0.04–3.25 ppm and 0.13–2.70 ppm, respectively (Cullers and Podkovyrov, 2000).

Based on the resulted geochemical data it is likely suggest that arenite associated with minor argillite composition of Early Paleozoic sequence of Shan Plateau (Maung Thein and Soe Win. 1970; Myint Lwin Thein et al., 1990; Myint Thein, 2014 pers. comm. in Maw Maw Win et al., 2016) or Mergui Group and older unexposed underlying rocks (Ridd and Watkinson, 2013) are primary contribution to the precursor sediments of the studied samples.

Source–Area Weathering

For each lithology the Chemical Index of Alteration CIA [= Al_2O_3 / (Al_2O_3 + CaO + Na_2O + K_2O) x 100] (Nesbitt and Young, 1982) values vary as follows: OZ samples (67–69), KB sample (62), SM1 sample (72) and SM2 samples (64–66). The SM1 sample is compared to the average shale (CIA = 70–75, Taylor and McLennan, 1985). The Chemical Index of Weathering CIW [= Al_2O_3/(Al_2O_3 + CaO + Na_2O) x 100] (Harnois, 1988) value for OZ, KB, SM1 and SM2 samples are 79–80, 76, 83 and 81–85. This is supported by the Index of Compositional Variability ICV [= (Fe_2O_3 + K_2O + Na_2O + CaO + MgO + TiO_2)/Al_2O_3] (Cox et al., 1995) value ranging from 1.28–1.30 for OZ samples, 1.12 for KB sample, 1.46 for SM1 sample and 1.37–1.45 for SM2 sample. These ranges indicate that the precursor rocks in the source area had undergone moderate to high degrees of chemical weathering.

In the A–CN–K diagram (Al_2O_3 – CaO ＋ Na_2O – K_2O), all samples are close to the boundary of plagioclase and alkali-feldspar except for SM1 sample, which is more Al rich indicating intense chemical weathering in the source region (Fig. 6a). In the A–CNK–FM diagram [(Al_2O_3 – (CaO＋Na_2O＋K_2O) – (Fe_2O_3＋MgO)], M1 value (M1 = FeO + MgO + Al_2O_3/K_2O + Na_2O + CaO) range 2.44–5.21 and M2 value (M2 = Al_2O_3/FeO + MgO) range 1.14–2.09 (Fig. 6b). This diagram shows the gradual chemical weathering trend. Fig. 6b shows that SM1 sample is plotted in the field A III and IV indicating intense weathered protolith and OZ and SM2 sample in field A III indicating a high weathering whereas KB02 sample show less weathered precursor rock.

Provenance and Tectonic Setting

The composition of major element or oxides was used to infer sedimentary provenance by the application of discriminant function analysis of Roser and Korsch (1988). In figure 7a, the samples are scattered in the quartzose sedimentary provenance field whereas KB02 sample is plotted in felsic igneous provenance field pointing to a major contribution of quarzose sedimentary rock to OZ and SM samples and felsic igneous materials to KB sample in their precursor sediments.

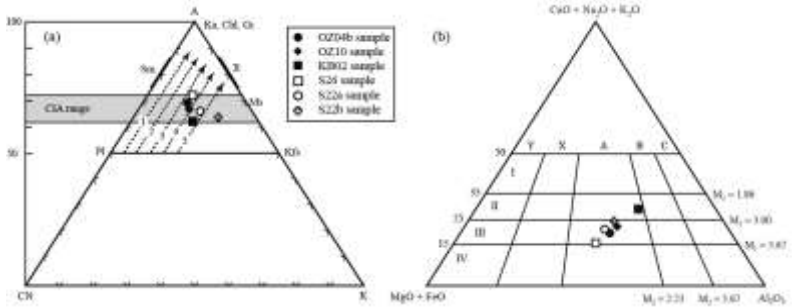

Figure 6 (a) A–CN–K diagram (after Nesbitt and Young, 1982) and (b) A–CNK–FM diagram for studied samples (after Englund and Jørgensen, 1973b). Weathering trends 1–5 are gabbro, tonalite, granodiorite, adamellite and granite (Fedo et al., 1997).

The present study was attempted to discriminate the tectonic setting based on the geochemical composition. The bivariate plot of logs K_2O/Na_2O against SiO_2/Al_2O_3 (Fig. 7b) and SiO_2 versus log K_2O/Na_2O (Fig. 7c) revealed that the samples are generally related to passive margin and active continental margin. Th–Co–Zr/10 tectonic discrimination diagram revealed that although some samples deviate from the distinctive setting, the source area is mostly of active continental margin (Fig. 7d).

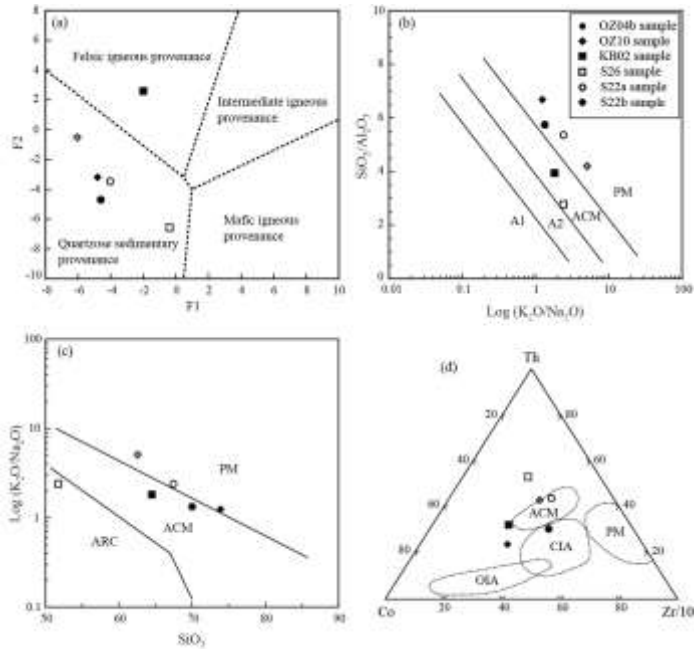

Figure 7 (a) Major element discriminant function diagram for studied samples (after Roser and Korsch, 1988), tectonic setting discrimination diagrams of (b) Log K_2O/Na_2O–SiO_2/Al_2O_3 (Maynard et al., 1982), (c) SiO_2–Log K_2O/Na_2O (Roser and Korsch, 1986), and (d) Th–Co–Zr/10 (Bhatia and Crook, 1986). A1 = arc setting; A2 = evolved arc setting; ACM = active continental margin; PM = passive margin; ARC = island arc margin; CIA = continental island arc; OIA = oceanic island arc.

Although some samples fall within a passive margin setting, it is likely that not all high-temperature rocks have such an origin. However, Searle et al. (1999; 2007) suggested that the western margin of Southeast Asia changed form a passive continental margin in the Permian with shallow, marine carbonate sedimentation, which continued throughout the Triassic and Lower Jurassic from the studies of Karakoram and Tibet, which was correlated in tectonic evolution with Mogok metamorphic belt. This was followed by an Andean-type convergent margin in Jurassic times, and magmatic activity during the India–Eurasian collision through Eocene–Miocene times. It is probable from the chemical compositions that the lithology and proportions of rock types vary and seem to record different tectonic settings and source area compositions, and certain tectonic settings do not necessarily generate rocks with distinct geochemical signatures (McLennan et al., 1990). More careful investigation of lithology followed by geochemical studies may still be needed to understand the metamorphism, protolith nature and tectonism of the Mogok metamorphic belt.

Conclusion

The Cenozoic Mogok metamorphic belt consists of metaigneous and metasedimentary rocks with various granitoid intrusions. The common mineral assemblages of gneiss samples are characterized by garnet + biotite + plagioclase + K-feldspar + quartz with cordierite and sillimanite in some samples. Based on the reported geothermobarometery the samples were formed under upper amphibolite to granulite facies conditions. Geochemical data were used to evaluate the possible protolith composition, source–area weathering, provenance and tectonic setting of the gneiss samples. Sagaing samples are more enriched in Fe compared with Onzon and Thabeikkyin samples. The major and minor oxides have a similar composition relative to the UCC with slight depletion of CaO, Na_2O and P_2O_5. Transition elements are comparable to average crustal content with slight enrichment of Ni. LILE elements scatter around with slight enrichment in Rb and marked depletion of Sr. HFSE elements show enrichment with marked Nb depletion. Evidences form major and trace element concentrations, ratios and use of various diagrams point to the derivation of Onzon samples and SM2 unit samples from psammitic composition mainly greywacke and SM1 unit sample from pelitic compositions except for Thabeikkyin sample, which has felsic igneous protolith. In addition, CIA, CIW and ICV values, and major element diagram have indicated the source areas had undergone moderate to high degree of weathering. Based on the major and trace element variation diagrams sediment deposition might have occurred at passive margin and active continental margin.

Acknowledgements

We would like to acknowledge late Dr. Myint Lwin Thein and his field party and also Dr. Myint Thein for allowing us to cite their unpublished field data of Onzon, Thabiekkyin and Sagaing areas. Thanks also due to petrology group of Nagoya University and colleagues at the Department of Geology, University of Magway for their comments and suggestions.

References

Argast, S. and Donnelly, T.W., (1987) "The chemical discrimination of clastic sedimentary components." *Journal of Sedimentary Petrology*, vol. 57, pp. 813–823.

Barley, M.E., Pickard, A.L., Khin Zaw, Rak, P. and Doyle, M.G., (2003) "Jurassic to Miocene magmatism and metamorphism in the Mogok metamorphic belt and the India-Eurasia collision in Myanmar." *Tectonics*, vol. 22, doi.10.1029/2002TC001398.

Bertrand, G., Rangin, C., Maluski, H. and Bellon, H., (2001) "Diachronous cooling along the Mogok metamorphic belt (Shan Scarp, Myanmar); the trace of the northward migration of the Indian syntaxis." *Journal of Asian Earth Sciences*, vol. 19, pp. 649-659.

Bertrand, G., Rangin, C., Maluski, H., Tin Aung Han, Ohn Myint, Win Maw and San Lwin. (1999) "Cenozoic metamorphism along the Shan Scarp (Myanmar); evidences for ductile shear along the Sagaing Fault or the northward migration of the eastern Himalayan syntaxis?" *Geophysical Research Letters*, vol. 26, pp. 915-918.

Bhatia, M.R. and Crook, K.A.W., (1986) "Trace element characteristics of graywackes and tectonic setting discrimination of sedimentary basins." *Contribution to Mineralogy and Petrology*, vol. 92, pp. 181-193.

Condie, K.C., (1993) "Chemical composition and evolution of the upper continental crust: contrasting results from surface samples and shales." *Chemical Geology*, vol. 104, pp. 1-37.

Cox, R., Lowe, D.R. (1995) "Compositional evolution of coarse elastic sediments in the south United States from 1.8 to 0.2 G.A. and implications for relationship between the development of crustal blocks and their sedimentary cover." *Journal of Sediment Research*, vol. 65, 477–494.

Cullers, R.L., and Podkovyrov, V.N., (2000) "Geochemistry of the Mesoproterozoic Lakhanda shales in southeastern Yakutia, Russia: implications for mineralogical and provenance control, and recycling." *Precambrian Research*, vol. 104, pp. 77–93.

Englund, J.O. and Jørgensen, P., (1973b) "A chemical classification system for argillaceous sediments and factors affecting their composition." *Geologiska Föreningens i Stockholm Förhandlingar*, vol. 95, pp. 87-97.

Fedo, C.M., Young, G.M., Nesbitt, H.W., (1997) "Paleoclimate control on the composition of the Paleoproterozoic Serpent formation, Huronian Supergroup, Canada, a greenhouse to icehouse transition." *Precambrian Research*, vol. 86, pp. 201-223.

Floyd, P.A., Leveridge, B.E., (1987) "Tectonic environment of the Devonian Gramscatho basin, south Cornwall: framework mode and geochemical evidence from turbiditic sandstones." *Journal of the Geological Society of London*, vol. 144, pp. 531–542.

Garcia, D., Coelho, J., Perrin, M., (1991) "Fractionation between TiO2 and Zr as a measure of sorting within shale and sandstone series (northern Portugal)." *European Journal of Mineralogy*, vol. 3, pp. 401–414.

Girty, G.H., Ridge, D.L., Knaack, C., Johnson, D., Al-Riyami, R.K., (1996) "Provenance and depositional setting of Paleozoic chert and argillite, Sierra Nevada, California." *Journal of Sedimentary Research*, vol. 66, pp. 107–118.

Gromet, L.P., Dymek, R.E., Haskin, L.A., Korotev, R.L., (1984) "The North American shale composite: its composition, major and trace element characteristics." *Geochimica et Cosmochimica Acta*, vol. 48, pp. 2469–2482.

Harnois, L., (1988) "The CIW index - a new chemical index of weathering." *Sedimentary Geology*, vol. 55, pp. 319–322.

Herron, M.M., (1988) "Geochemical classification of terrigenous sands and shales from core of log data." *Journal of Sedimentary Petrology*, vol. 58 (5), pp. 820–829.

Maung Thein and Soe Win (1970) "The metamorphic petrology, structure and mineral resources of the Shantung–U-Thandawmywet Range, Kyaukse District." *Burma Science and Technology Journal*, vol. 3, pp. 487–514.

Maw Maw Win, Enami, M. and Kato, T., (2016) "Metamorphic conditions and CHIME monazite ages of Late Eocene to Late Oligocene high-temperature Mogok metamorphic rocks in central Myanmar." *Journal of Asian Earth Sciences*, vol. 117, pp. 304-316.

Maynard, J.B., Valloni, R., Yu, H., (1982) "Composition of modern deep sea sands from arc-related basins." *Geological Society of London*, Special Publication, vol. 10, pp. 551-561.

McLennan, S.M., (2001) "Relationships between the trace element composition of sedimentary rocks and upper continental crust." *Geochemistry, Geophysics, Geosystems*, 2 (2000GC000109 (electronic publication).

McLennan, S.M., Taylor, S.R., McCulloch, M.T., Maynard, J.B., (1990) "Geochemical and Nd–Sr isotopic composition of deep-sea turbidites: crustal evolution and plate tectonic associations." *Geochimica et Cosmochimica Acta*, vol. 54, pp. 2015–2050.

Mitchell, A.H.G., Myint Thein Htay, Htun, K.M., Myint Naing Win, Thura Oo and Tin Hlaing (2007) "Rock relationships in the Mogok metamorphic belt, Tatkon to Mandalay, central Myanmar." *Journal of Asian Earth Sciences*, vol. 29, pp. 891-910.

Myint Lwin Thein, Ohn Myint, Sun Kyi and Phone Nyunt Win (1990) "Geology and stratigraphy of the metamorphosed Early Paleozoic rocks of the Mogok-Thabeikkyin-Singu-Madaya Areas." Staff report, no. 98, pp. 24, Applied Geology Department, University of Yangon.

Nesbitt, H. W. and Young, G. M., (1984) "Prediction of some weathering trends of plutonic and volcanic rocks based on thermodynamic and kinetic considerations." *Geochimica et Cosmochimica Acta*, vol. 48, pp. 1523–1534.

Ridd, M.F., and Watkinson, I., (2013) "The Phuket-Slate Belt terrane: tectonic evolution and strike-slip emplacement of a major terrane on the Sundaland margin of Thailand and Myanmar." *Proceedings of the Geologists Association*, vol. 124, pp. 994-1010.

Roser, B.P., Korsch, R.J., (1986) "Determination of tectonic setting of sandstone-mudstone suites using SiO_2 content and K_2O/Na_2O ratio." *Journal of Geology*, vol. 94, pp. 635-650.

Roser, B.P., Korsch, R.J., (1988) "Provenance signatures of sandstone-mudstone suites determined using discriminant function analysis of major-element data." *Chemical Geology*, vol. 67, pp. 119–139.

Rudnick, R.L., Gao, S., (2003) *The composition of the continental crust*. In: Rudnick, R.L. (Ed.), The Crust. Elsevier-Pergamon, Oxford, pp. 1–64.

Searle, M.P., Khan, M.A., Fraser, J.E., and Gough, S.J., (1999) "The tectonic evolution of the Kohistan-Karakoram collision belt along the Karakoram Highway transect, north Pakistan." *Tectonics*, vol. 18, pp. 929-949.

Searle, M.P., Noble, S.R., Cottle, J.M., Waters, D.J., Mitchell, A.H.G., Tin Hlaing and Horstwood, M.S.A., (2007) "Tectonic evolution of the Mogok metamorphic belt, Burma (Myanmar) constrained by U-T-/Pb dating of metamorphic and magmatic rocks." *Tectonics*, vol. 26, TC3014.

Shaw, D.M., (1956) "Geochemistry of Pelitic Rocks. Part III: Major Elements and General Geochemistry," *Geological Society of American Bulletin*, vol. 67, pp. 913–934.

Shaw, D. M., (1972) "The origin of the Apsley gneiss, Ontario." *Canadian Journal of Earth Sciences*, vol. 9, pp.18–35.

Taylor, S.R. and McLennan, S.M., (1985) *The Continental Crust: Its Composition and Evolution*. Blackwell Scientific Publishers, Oxford.

Varga, A.R., Szakmány, G., (2004) "Geochemistry and provenance of the upper carboniferous sandstones from borehole diósviszló-3 (Téseny Sandstone Formation, SW hungary)." *Acta Mineralogica–Petrographica*, Szeged vol. 45/2, pp. 7–14.

Whitney, D.L. and Evans, B.W., (2010) "Abbreviations for names of rock–forming minerals." *American Mineralogist*, vol. 95, pp. 185-187.

Wimmenauer, W. (1984) "Das prävariskische Kristallin im Schwarzwald." *Fortschritte der Mineralogie*, 62 (Beiheft 2), pp. 69–86.

Ye Kyaw Thu, Enami, M., Kato, T. and Tsuboi, M., (2017) "Granulite facies paragneisses from the middle segment of the Mogok metamorphic belt, central Myanmar." *Journal of Mineralogical and Petrological Sciences*, vol. 112, pp. 1–19.

Ye Kyaw Thu, Maw Maw Win, Enami, M. and Tsuboi, M., (2016) "Ti-rich biotite in spinel and quartz-bearing paragneiss and related rocks from the Mogok metamorphic belt, central Myanmar." *Journal of Mineralogical and Petrological Sciences*, vol. 111, pp. 270–282.

Yonemura, K., Osanai, Y., Nakano, N., Adachi, T., Charusiri, P. and Tun Naing Zaw, (2013) "EPMA U-Th-Pb monazite dating of metamorphic rocks from the Mogok Metamorphic Belt, central Myanmar." *Journal of Mineralogical and Petrological Sciences*, vol. 108, pp. 184-188.